Biosensors and Bioelectronics 261 (2024) 116444

Contents lists available at ScienceDirect

Biosensors and Bioelectronics

journal homepage: www.elsevier.com/locate/bios

Increasing the stability of electrolyte-gated organic synaptic transistors for neuromorphic implants

Seung-Woo Lee [a,1], Somin Kim [a,1], Kwan-Nyeong Kim [a,1], Min-Jun Sung [a], Tae-Woo Lee [a,b,*]

[a] Department of Materials Science and Engineering, Seoul National University, Seoul, 08826, Republic of Korea
[b] Interdisciplinary Program in Bioengineering, Institute of Engineering Research, Research Institute of Advanced Materials, Soft Foundry, Bio-MAX Institute, Seoul National University, Seoul, 08826, Republic of Korea

ARTICLE INFO

Keywords:
Implantable bioelectronics
Neuromorphic electronics
Organic synaptic transistor
Long-term stability
Neuroprosthetics
Organic nervetronics

ABSTRACT

Electrolyte-gated organic synaptic transistors (EGOSTs) can have versatile synaptic plasticity in a single device, so they are promising as components of neuromorphic implants that are intended for use in neuroprosthetic electronic nerves that are energy-efficient and have simple system structure. With the advancement in transistor properties of EGOSTs, the commercialization of neuromorphic implants for practical long-term use requires consistent operation, so they must be stable *in vivo*. This requirement demands strategies that maintain electronic and ionic transport in the devices while implanted in the human body, and that are mechanically, environmentally, and operationally stable. Here, we cover the structure, working mechanisms, and electrical responses of EGOSTs. We then focus on strategies to ensure their stability to maintain these characteristics and prevent adverse effects on biological tissues. We also highlight state-of-the-art neuromorphic implants that incorporate these strategies. We conclude by presenting a perspective on improvements that are needed in EGOSTs to develop practical, neuromorphic implants that are long-term useable.

1. Introduction

Restoration of compromised neural functions is crucial to enhance patients' quality of life and to extend their lifespan. Neuroprosthetic electronic nerves can provide a solution by processing, interpreting, and rerouting bio-signals to reinstate lost neural functions (Kato et al., 2019; Lorach et al., 2023). However, existing digital systems are inflexible and use excessive energy, so they are unsuitable for portable and long-term implantable applications. To overcome these limitations, biomimetic neuroprosthetic electronic nerves (i.e., neuromorphic implants) present a promising solution with energy-efficient operation and a simple system structure (Go et al., 2022; Kim et al., 2022; Park et al., 2020). These devices are designed to mimic analog processing by biological neural networks. Development of such devices must realize portable artificial nerves that establish a biologically-compatible connection with biological nerves, and that can be powered for long times by wearable batteries.

Biological synapses transmit spike signals to the postsynaptic neuron by diffusion of chemicals across the synaptic cleft. The spike responses of the postsynaptic neuron (e.g., response time, intensity of generated spikes) can vary predictably depending on experience and environment; this phenomenon is called synaptic plasticity (Abbott and Regehr, 2004; Citri and Malenka, 2008; Zucker and Regehr, 2002).

To emulate the functionality of biological nerves, artificial synaptic devices must have both memory and signal-processing abilities simultaneously. Electrolyte-gated organic synaptic transistors (EGOSTs), particularly with ion-permeable organic channels, operate by exploiting the interaction of organic semiconductors or conductors with ions to control the electrochemical doping state of the channel. This mechanism resembles the neurotransmitter-receptor reactions in biological synapses, and thereby enables emulation of signal-transmission behaviors of biological nerves as electrical outputs. By modifying the molecular design (Kim et al., 2023) and microstructure of organic channels (Go et al., 2020; Seo et al., 2019), EGOSTs can be made to have versatile synaptic plasticity. Recently, EGOSTs that mimic the short-term plasticity of biological synapses have enabled emulation of the biological reflex arc of a cockroach, and subsequent movement of a cockroach leg in response to the sensory signals (Kim et al., 2018). Moreover, EGOSTs with long-term memory capability have been applied as memory units for the classification of physiological signals by artificial intelligence

* Corresponding author. Department of Materials Science and Engineering, Seoul National University, Seoul, 08826, Republic of Korea.
E-mail address: twlees@snu.ac.kr (T.-W. Lee).
[1] Seung-Woo Lee, Somin Kim, and Kwan-Nyeong Kim contributed equally to this work.

https://doi.org/10.1016/j.bios.2024.116444
Received 11 March 2024; Received in revised form 16 May 2024; Accepted 27 May 2024
Available online 28 May 2024

(Dai et al., 2022a). Therefore, EGOSTs are appropriate for the development of neuromorphic implants that can in principle emulate neural networks in peripheral and central nervous systems, and can thereby provide a suitable approach to potentially replace various signal-processing functions of the human nervous system.

However, practical long-term use of neuromorphic implants remains a challenge. Several instabilities of EGOSTs can degrade their functions of EGOSTs (Fig. 1): (1) They are mechanically unstable when subjected to repetitive flexing and stretching, as would occur when the user moves. (2) They are environmentally unstable due to chemical reactions between the device and the physiological milieu. (3) They are operationally unstable due to undesirable changes during the electrochemical processes.

EGOSTs with ion-permeable channel can have high volumetric capacitance; this characteristic allows them to function as transistors capable of high amplification at low operation voltages, and gives them versatile synaptic plasticity from short-term to long-term (Lee et al., 2022b). *In vivo*, the electronic and ionic transport characteristics of EGOSTs, particularly of organic channel materials, can be easily degraded, and this change compromises the long-term operation of neuromorphic implants and triggers undesired responses, which could harm the human host. Therefore, the development of neuromorphic implants that use EGOSTs to operate reliably and accurately for sufficient time requires materials and device-engineering strategies to enhance transistor parameters of EGOST while simultaneously ensuring stability *in vivo* by preventing degradation of electronic and ionic transport properties in the organic channels.

This review introduces the working mechanisms, transistor parameters, and synaptic behaviors of EGOSTs. Then it explores strategies to increase the mechanical stability, environmental stability, and operational stability of EGOSTs; these improvements are crucial for maintaining electronic and ionic transport in the application of EGOSTs for neuromorphic implants. Then the review highlights state-of-the-art research in neuromorphic implants that have used these strategies. To conclude, the review addresses the improvements that must be achieved in EGOSTs to enable neuromorphic implants that are both practical and suitable for long-term use.

2. EGOSTs for the application of neuromorphic implants

For the development of neuromorphic implants, EGOSTs must have excellent transistor parameters, such as high transconductance g_m, high ratio of 'on' current I_{on} to 'off' current I_{off}, and low operating voltage, while having synaptic plasticity that can vary from short-term to long-term. In this section, we introduce the working mechanisms of EGOSTs and their classification according to dependence on synaptic plasticity. Then we explain the transistor parameters and synaptic behaviors in the spike responses of EGOSTs.

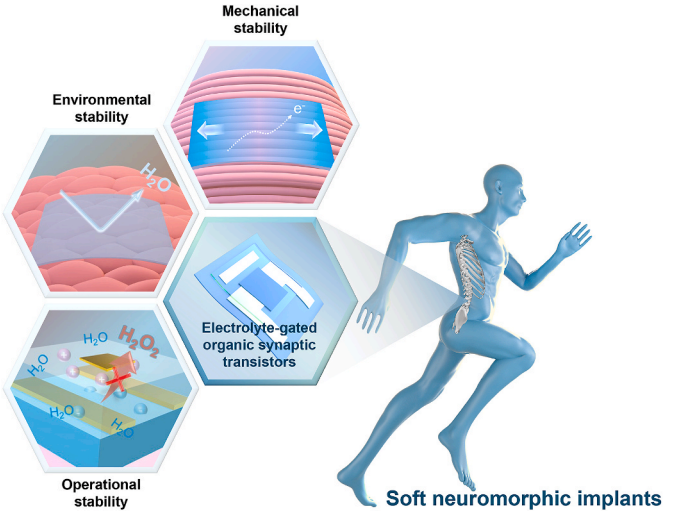

Fig. 1. Schematics of various stabilities required for the successful implementation of EGOSTs in soft neuromorphic implants.

EGOSTs are three-terminal devices that can modulate the conductance of an ion-permeable channel by using gate bias to induce electrochemical doping and de-doping of organic channels; these changes generate electrical outputs (Fig. 2a). When a pre-synaptic voltage spike V_G is applied to the gate electrode, mobile ions migrate toward the electrolyte-semiconductor interface, where they form an electric double layer and subsequently penetrate the organic channel materials; these processes increase the conductance of the organic channel due to the injection of holes (p-type) or electrons (n-type). After the pulse ends, the ions diffuse back to their original distribution, and the doping state and conductivity of the organic channel return to their initial levels.

By modulating the electronic and ionic transport in EGOSTs, the volatility of the response can be controlled to emulate the synaptic plasticity of biological synapses. EGOSTs can be classified into three types according to the volatility of their electrical response to spiking signals: short-term-dominant EGOSTs, long-term-dominant EGOSTs, and non-volatile EGOSTs (Fig. 2b). Although a quantitative criterion for this classification has not been established, this qualitative classification can differentiate among the bio-inspired functions of EGOSTs and guide the selection of synaptic devices in hardware-based implementations of neural networks.

EGOSTs combine synaptic characteristics with a transistor's amplification and switching functions. By measuring the transfer curve of EGOSTs, these functionalities can be evaluated (Fig. 2c). The novelty of EGOSTs lies in high volumetric capacitance due to porous organic channels; therefore the EGOSTs can function as transistors that are capable of high amplification at low operating voltage (Liu et al., 2024; Rivnay et al., 2018). This amplification capability of EGOSTs can be evaluated by the g_m and I_{on}/I_{off} of their transfer curves. With these advantages, the synaptic plasticity dependence can be characterized by the hysteresis window ΔV_{Hys} that also appears in the transfer curves.

I_{on}/I_{off} in the transfer curve is the ratio of the maximum current I_{on} in the 'on' state to the current I_{off} in the 'off' state (i.e., undoped state). A high I_{on}/I_{off} can reduce the effect of noisy background during amplifying transistor operations, and thereby enable signal processing with a high signal-to-noise ratio that can increase accuracy in sensor-data acquisition.

The parameter g_m quantifies the EGOST's responses to changes in input voltage. An EGOST that has high g_m can achieve the desired signal modulation with low operating voltage and low energy consumption. g_m is calculated from the slope of the transfer curve as equation (1), where I_D is drain current, V_G is gate voltage, μ is carrier mobility, C^* is the volumetric capacitance of the channel, W, L, and d are respectively channel width, length, and thickness, and V_{Th} is the threshold voltage. Generally, g_m is normalized to device geometry as equation (2), where NR means 'normalized', to ensure the accurate comparison between various devices (Inal et al., 2017; Ohayon et al., 2023; Wang et al., 2023a).

$$g_m = \frac{\partial I_D}{\partial V_G} = \mu C^* \frac{Wd}{L}(V_{Th} - V_G) \quad (1)$$

$$g_m(NR) = g_m \frac{L}{Wd} \quad (2)$$

The figure of merit μC^* governs g_m and captures the steady-state ionic/electronic transport properties of the channel materials. A high μC^* requires efficient electronic transport and strong ionic-electronic coupling. However, high C^* (i.e. efficient ion infiltration and charging) can induce unwanted charge traps and structural changes in the organic channel that impede charge transport, and thereby decrease μ. Therefore, to maximize the μC^*, engineering of materials and devices

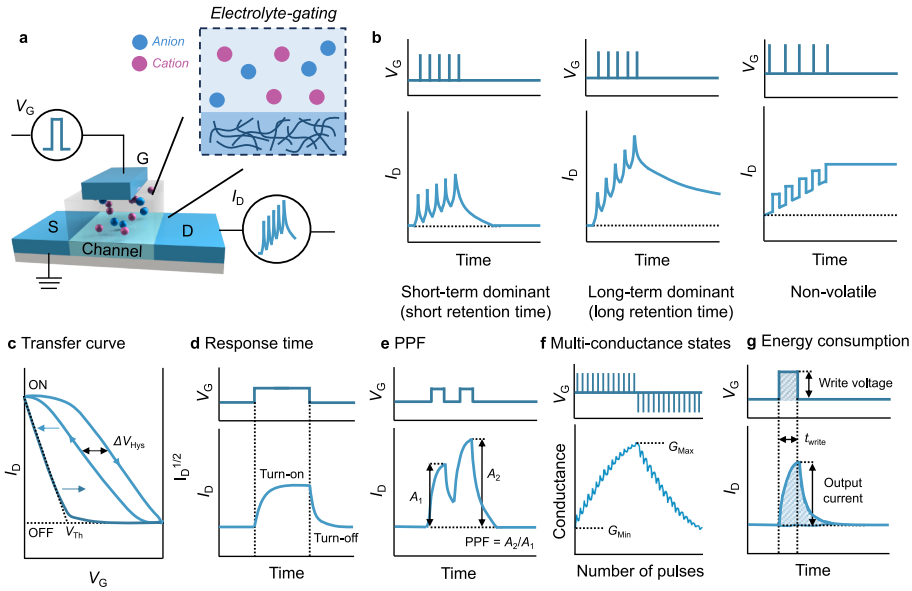

Fig. 2. An overview of the structure, working mechanisms, and electrical responses in EGOSTs. **a)** Structure and working mechanisms of EGOSTs. Electrical responses are generated by gate bias-induced electrochemical doping and de-doping of organic channels. **b)** Classification of EGOSTs according to dependence on synaptic plasticity. Depending on the volatility of their electrical response to spiking signals, they are classified into short-term dominant, long-term dominant, and non-volatile EGOSTs. **c)** Transistor performance (g_m, I_{On}/I_{Off}, V_{Th}, ΔV_{Hys}) is evaluated from the response of I_D against a double-sweep of V_G (transfer curve). **d)** Switching performance (τ_{ON}, τ_{OFF}) is evaluated from the response of I_D against the step of V_G. **e)** The paired-pulse facilitation (PPF) index is the ratio of I_D (A_2/A_1) from consecutive V_G spikes. **f)** Consecutive V_G spikes update channel conductance in multi-conductance states in dynamic range (G_{max}/G_{min}). **g)** Energy consumption from a single write voltage spike is calculated by $V_G \times I_G \times t_{write} + V_D \times I_D \times t_{read}$.

must achieve an ideal balance between them (Tropp et al., 2023; Wang et al., 2024).

The hysteresis window ΔV_{Hys} is the difference between the voltage at which I_D reaches half the I_{on} during the forward sweep, and the voltage at which I_D reaches half the I_{on} during the backward sweep. Large ΔV_{Hys} implies that further spike responses will demonstrate memory. ΔV_{Hys} can used to compare whether EGOSTs are short-term-dominant, long-term-dominant, or non-volatile.

EGOSTs undergo transistor switching, and to mimic synaptic plasticity, the interaction between organic channels and ions should be controlled to modulate the spike response time and match it to the response time of target biological synapses (Fig. 2d). For example, the turn-on time τ_{ON} could be modulated by adjusting the hydrophilicity matching between organic semiconductors and ions. Poly(3-hexylthiophene-2,5-diyl) (P3HT) is an organic semiconductor with hydrophobic alkyl side chains; it could achieve faster turn-on (τ_{ON} = 460 ms) when used with the relatively hydrophobic bis(trifluoromethanesulfonyl)imide (TFSI) anion than with hydrophilic tetrafluoroborate (BF_4) anion (τ_{ON} = 1620 ms) (Wu et al., 2023b).

Decoding of temporarily correlated spike signals in EGOSTs is required for information processing, filtering, and other actions. Paired-pulse facilitation (PPF) is crucial for decoding temporal information (Liu et al., 2015) and is represented by the PPF index A_2/A_1 in response to the consecutive input spikes, where A_1 is the amplitude of the response to the first voltage spike, and A_2 is the amplitude of the response to the second spike (Fig. 2e). This index can undergo concurrent slow and fast decay responses coherent with the facilitation behavior in biological synapses (Ji et al., 2021). This behavior of the EGOSTs can be exploited to emulate the responses of the peripheral nervous system, such as somatosensory peripheral nerves, which could realize a hybrid bioelectronic reflex arc that uses a neuromorphic implant (Kim et al., 2018).

Intelligent processing and computing rely on the long-term plasticity (LTP) of EGOSTs, which can realize high-level processing such as recognition and classification. For example, regarding sensory processing, the use of non-volatile EGOSTs enabled robots to learn from successive stimuli, and to exploit experience to adjust spike responses to subsequent stimuli (Krauhausen et al., 2021). This intelligent function of a single EGOST is crucial for simplifying the system architecture of artificial nerves, and for minimizing energy consumption by eliminating the need for additional circuitry.

To quantitatively evaluate the precision of EGOST-based hardware neural networks, the multi-conductance states are measured by applying consecutive potentiation and depression spike voltages (Fig. 2f). In these multi-conductance states, the dynamic range is obtained from the conductance ratio from its minimum value G_{Min} to its maximum value G_{Max}. High-accuracy neuromorphic computing requires a wide dynamic range G_{Max}/G_{Min} and a large number of conductance states (Lee and Lee, 2019; Park and Lee, 2021) to improve tolerance to device-to-device variations. Furthermore, to make this weight-update process accurate and repeatable, the multi-conductance states should be linear and symmetrical (Gumyusenge et al., 2021; van de Burgt et al., 2018).

Implantable devices currently require external power sources, and therefore must have minimal energy consumption to permit long-term use. Low energy consumption by implantable electronic devices can reduce heat generation which could cause tissue damage and patient discomfort (Bazaka and Jacob, 2013). The energy consumption of the EGOSTs can be calculated by summing the energy consumption in the programming step and the reading step as equation (3) (Fig. 2g). I_G is usually negligible compared to I_D, so for EGOSTs that have low I_G, this calculation can be simplified to equation (4).

$$V_G \times I_G \times t_{write} + V_D \times I_D \times t_{read} \quad (3)$$

$$V_D \times I_D \times t_{read} \quad (4)$$

Therefore, EGOSTs that operate in accumulation mode, in which input spikes increase the initial channel conductance, can have lower energy consumption than EGOSTs that operate in depletion mode, in which input spikes decrease the initial channel conductance (Keene et al., 2020; Lee et al., 2021).

Material and device engineering can also reduce the energy consumption of EGOSTs. For example, ultralow energy consumption of ~1.23 fJ per synaptic event, which is comparable to the <10 fJ per

synaptic event energy consumption of biological synapses, was achieved by downscaling the organic semiconductor channel to 300 nm by nanowire printing (Xu et al., 2016). Thus, nanoscale EGOSTs that operate in accumulation mode can be promising candidates for realizing low-power implantable applications of EGOSTs.

3. Strategies to increase the stability of EGOSTs

When used as components in devices that mimic the biological functions of a living organism, EGOSTs must not degrade in that environment; otherwise, they cannot operate accurately or retain their functions over the long term. In particular, the charge-transport characteristics of EGOSTs are governed by their channel materials, so their stability can determine the suitability of EGOSTs as neuromorphic implants. In this section, we introduce recent strategies to increase the mechanical, environmental, and operational stability of EGOSTs by focusing on the transport of electrons and ions. In addition, since research on EGOST is in its early stages, we comprehensively cover various transistors such as field-effect transistors, organic electrochemical transistors, etc., that have organic channels.

3.1. Mechanical stability

The mismatch between the soft mechanical properties of biological tissues and the rigid properties of electronic components can cause inflammatory reactions and failure of neuromorphic implants during their movement caused by autonomous or intentional movements of biological organs or muscles (Sunwoo et al., 2021). Moreover, degradation of the initial implant operation could induce reactions that harm the recipient. Therefore, stable and long-term implantable electronics require materials and devices that have mechanical properties that are compatible with biological tissues.

3.1.1. Intrinsic methods

Charge transport is primarily determined by the organic channel, so research has focused on increasing the stretchability of the organic channel while preserving charge transport (Seo et al., 2021; Zheng et al., 2022). EGOSTs must be stretchable to ~70% to prevent tissue damage and device failure during daily body movements, as well as to minimize the implant rejection mediated by the immune system (Li et al., 2021). Imparting stretchability to all component materials of EGOSTs (e.g., substrate, electrolyte, organic channel, electrode) can be beneficial by achieving uniform and effective distribution of mechanical stress along attached biological tissues (Wang et al., 2023c).

The conjugated polymer/elastomer phase separation–induced elasticity (CONPHINE) method separates the polymer semiconductor and elastomer phases, and can significantly increase both the carrier mobility and stretchability of polymer films to overcome the brittle nature of conjugated polymers that have a crack onset strain of ~10% (Fig. 3a) (Xu et al., 2017). In the CONPHINE film, diketopyrrolopyrrole (DPP)-based polymer semiconductor, namely diketopyrrolopyrrole bithiophene thienothiophene (DPPT-TT) aggregate into nanofibril structures embedded within a poly(styrene-*b*-(ethylene-*co*-butylene)-*b*-styrene) (SEBS) matrix rather than within conventional semicrystalline bulk film. This morphological change releases the applied mechanical stress to the DPPT-TT chains by the elastomer matrix and fibril structure while maintaining the charge transport with high aggregation of DPPT-TT. To fabricate a stretchable transistor, carbon nanotube (CNT) was used as source, drain,

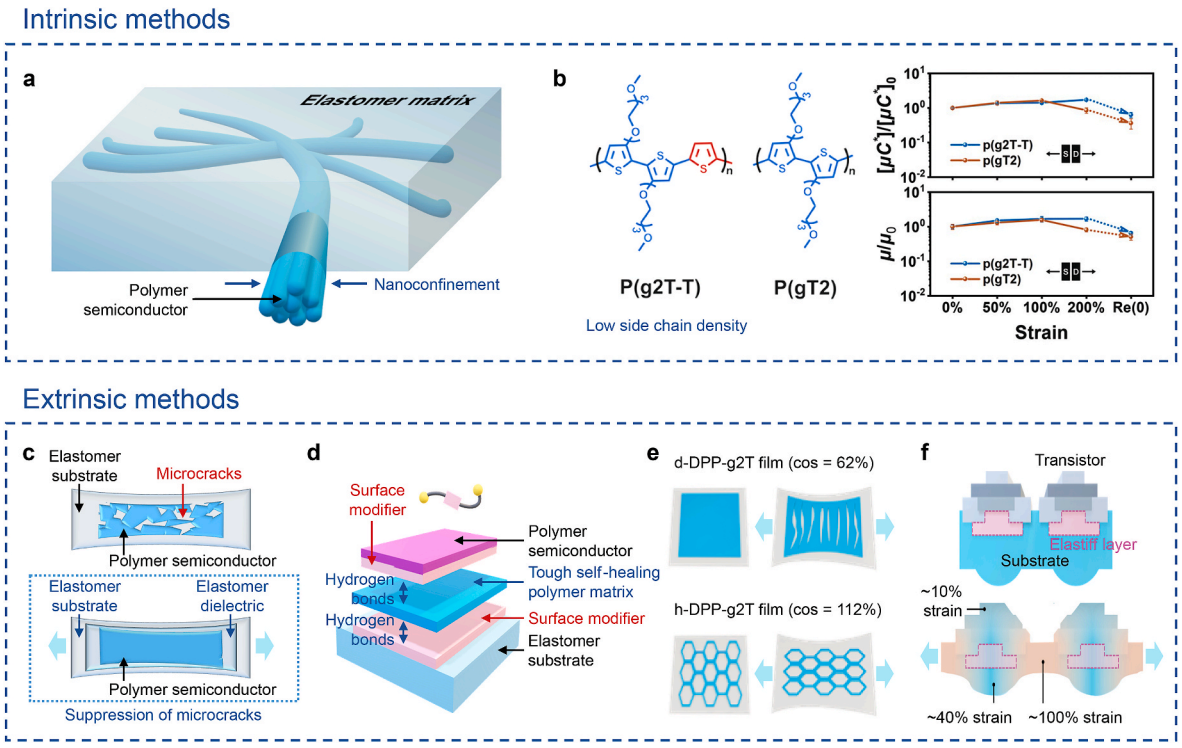

Fig. 3. Methods to increase mechanical stability of EGOSTs. **a)** Morphology of nanoconfined polymer semiconductor in the elastomer matrix. The elastomer matrix released the mechanical stress, and polymer semiconductor nanofibrils maintained charge transport. Reproduced with permission (Xu et al., 2017). Copyright 2017, AAAS. **b)** Chemical structures of p(g2T-T) and p(gT2) and change in μ and μC^* under strain. Less side-chain-attached backbone architecture increased mechanical stability. Reproduced with permission (Y. Dai et al., 2022b). Copyright 2022, Wiley-VCH. **c)** Polymer semiconductor on elastomer substrate and ESE stack. ESE stack suppressed the formation of microcracks. Reproduced with permission (Shim et al., 2023). Copyright 2023, Springer Nature. **d)** Tough-interface between semiconducting thin film and elastomer substrate. Dynamic hydrogen bonding between the SM and SHP layers dissipates energy. Reproduced with permission (Kang et al., 2022). Copyright 2022, Springer Nature. **e)** Dense and porous honeycomb-structured DPP-g2T film. Pore deformation of the honeycomb structure increased the stretchability. Reproduced with permission (Chen et al., 2022). Copyright 2022, Springer Nature. **f)** Elastiff layer. The strain applied on the active regions was reduced, enabling the strain-insensitive operation. Reproduced with permission (Wang et al., 2021). Copyright 2022, Springer Nature.

and gate electrodes, and SEBS was used as the dielectric, substrate, and encapsulation layers. As a result, the transistor had high carrier mobility with minimal degradation from 0.59 $cm^2\ V^{-1}\ s^{-1}$ under no strain to 0.55 $cm^2\ V^{-1}\ s^{-1}$ under 100% strain. The carrier mobility of the transistor decreased by only ~70% after >1000 strain cycles at 25% strain. The morphological changes induced by the CONFINE method could overcome the limitations imposed by the polymer semiconductors that are brittle.

Without any loss of carrier mobility by insulating additives, the chemical design of the polymer semiconductor moiety allows it to maintain stable charge transport and electrochemical reaction capabilities even under 100% strain in an electrochemical transistor (Fig. 3b) (Dai et al., 2022b). The authors synthesized poly(2-(3,3′-bis (2-(2-(2-methoxyethoxy)ethoxy)ethoxy)-[2,2′-bithiophen]-5)yl thiophene) (p(g2T-T)), which is a redox-active organic semiconductor that has an electron-rich thiophene backbone that favors electrochemical doping and a polar glycol side that facilitates ion transport. In the repeating unit of p(g2T-T), a thiophene unit without side chains can reduce the density of side-chain substitutions compared to backbones that have fully-attached side chains, so π-π stacking densifies in the thiophene backbone. This less side-chain-attached backbone architecture favors chain rearrangement from mixed in-plane and out-of-plane lamellar to in-plane dominant lamellar, and can dissipate strain and provide crack-free stretchability up to 200% uniaxial strain. Stretchable electrochemical transistors that exploit p(g2T-T) were fabricated using gold nanowires as the source and drain electrodes, aqueous NaCl as the electrolyte, and Ag/AgCl as the gate electrode. This device had efficient charge transport along the redox-active backbone, and therefore achieved a high $g_m(NR) = 223\ S\ cm^{-1}$, which is the highest reported for stretchable electrochemical transistors. When stretched parallel to charge transport, this device lost about 50% of its $g_m(NR)$ when subjected to 100% strain, and lost about 50% of I_{on} after 1000 cycles of stretching to 100% strain.

Although the stretchability of the organic channel has been significantly increased, the degradation of device operation remains significant. Therefore, strategies must be developed to achieve stretchable devices that have electrical characteristics that are not sensitive to stretching.

3.1.2. Extrinsic methods

These strategies use structural approaches, such as wavy or island structures or by interface design to reduce the degradation caused by mechanical deformation (Lee et al., 2018; Yao et al., 2023). By modifying the structure and device design, these methods can complement intrinsic methods.

To enable the fabrication of a stretchable transistor that uses a brittle polymer semiconductor, the polymer film was sandwiched between elastomer layers to form an elastomer-semiconductor-elastomer (ESE) stack (Fig. 3c) (Shim et al., 2023). The poly[(N,N′-bis(2-octyldodecyl)-naphthalene-1,4,5,8-bis(dicarboximide)-2,6-diyl)-alt-5,5′-(2,2′-bithiophene)] (P(NDI2OD-T2) or N2200) on polydimethylsiloxane (PDMS) showed numerous cracks under 50% uniaxial strain due to brittle nature. When the ESE structure was formed using polyurethane (PU) on N2200, crack formation at the same amount of strain was effectively suppressed, and N2200 showed significantly reduced normalized resistance change ($\Delta R/R_0$) ~ 3.3 compared to pristine N2200 on PDMS, which had $\Delta R/R_0$ ~ 17. This excellent inhibition of crack formation is caused by the generation of competing shear stress and delocalized stress concentration in multilayer stacked geometry, so that critical crack length increases. To fabricate a stretchable transistor even using a brittle organic semiconductor, N2200 was used as the organic channel, and silver nanowires were used as the source and drain electrodes on PDMS; the PU dielectric was coated on the top of N2200 to form an ESE structure. The field-effect mobility dropped from 0.22 $cm^2\ V^{-1}\ s^{-1}$ to 0.12 $cm^2\ V^{-1}\ s^{-1}$ under 50% uniaxial strain and partially recovered to 0.14 $cm^2\ V^{-1}\ s^{-1}$ after release. Despite the maximum strain being smaller than that of the target biological tissues, this method could provide a simple solution to use brittle organic channels for stretchable devices.

Highly stretchable transistors that use non-stretchable polymer semiconductors and conductors can be achieved by toughening the interfaces between substrate and dielectric, and between dielectric and organic channel (Fig. 3d) (Kang et al., 2022). This tough-interface design has a surface modifier (SM)/self-healable polymer (SHP)/SM structure; SM can covalently bond with any polymer due to its perfluorophenylazide or benzophenone moieties at the ends of a flexible polydimethylsiloxane chain. SM was directly spray-coated on an organic channel DPP-TT film fabricated on octadecyltrichlorosilane (OTS)-treated SiO_2, then a mixture of SM and SHP dielectric was spin-coated on the top of SM, resulting in the formation of PDMS/SM/SHP/SM/DPP-TT structure by transferring the layer on PDMS. In this structure, non-covalent interaction of SM/SHP/SM interface and covalent interactions of the SM with substrate and organic channel can occur. Non-covalent bonding by dynamic hydrogen bonding between the SM and SHP layers effectively dissipates energy, delaying the initiation of cracks on DPP-TT from about 40% strain on bare PDMS to about 110%. With CNT stretchable source and drain electrodes, the field-effect mobility of the organic transistor degraded by ~30% from 0.73 (±0.14) $cm^2\ V^{-1}\ s^{-1}$ without strain to 0.53 (±0.16) $cm^2\ V^{-1}\ s^{-1}$ under 100% strain. The use of this tough-interface approach with other brittle polymer semiconductors such as diketopyrrolopyrrole-thienyl-vinyl-thiophene (DPP-TVT), Isoindigo-2T, and P3HT, eliminated observable cracking under 100% uniaxial strain. This interface for a conducting polymer on PDMS showed no cracks under 40% strain. The tough-interface design strategy can overcome the mechanical limitations of existing organic channel materials while realizing superior stretchability, thereby expanding the range of available materials.

Despite the advances in stretchable transistors using bulk film of organic channel materials, the geometrical parameters of transistors change during stretching, so their electrical characteristics inevitably degrade. To address this problem, porous honeycomb-structured organic channels can be formed (Fig. 3e) (Chen et al., 2022). DPP-g2T amphiphilic polymer was dissolved in CF/MeOH and spin-coated onto a poly(vinyl alcohol) (PVA) sacrificial layer under 90% relative humidity to form a honeycomb structure of DPP-g2T. In this film, the deformation of pores in the honeycomb structure increases the stretchability of the film, and increases the crack-onset strain from 62 (±7.4)% for the dense film to 112 (±4.0)% for honeycomb-structured DPP-g2T. Moreover, rigid electrochemical transistors that use honeycomb DPP-g2T film showed negligible loss of switching ability following 1500 redox cycles. To fabricate the stretchable EGOSTs, SEBS substrate was stretched biaxially then gold source and drain electrodes and honeycomb DPP-g2T film were transferred onto the substrate, and aqueous KPF_6 electrolyte and Ag/AgCl gate electrode were applied after the release. This device had $g_m = 1.94$ (±0.03) mS at 0% strain and its decrease was negligible until 90% strain. After 1000 stretching cycles at 30% strain, g_m dropped by 13% when the strain was in the parallel direction, and by 8% when the strain was in the perpendicular direction. With these mechanically stable properties, EGOSTs had highly-reliable synaptic plasticity, with a decrease in the PPF index of only 4% at 60% biaxial strain. By implementing the geometric design of the channel film, mechanically durable synaptic plasticity of EGOSTs has been achieved and has the potential to complement intrinsic approaches for the fabrication of stretchable EGOSTs to improve mechanical durability.

Despite a significant improvement in mechanical stability, the additional fabrication process for geometrical modification of the channel film could potentially reduce the number of transistors per unit area (Li et al., 2021). Heterogeneously patterned regions that have high elastic modulus within an elastomer substrate (elastiff layers) can be used to create a strain-insensitive stretchable transistor array that has a high device density of 340 transistors cm^{-2} (Fig. 3f) (Wang et al., 2021). A stretchable transistor array was fabricated using azide-cross-linked SEBS dielectric layer, DPP-based CONPHINE semiconductor channel, and CNT as the source and drain electrodes patterned on dextran

water-soluble sacrificial layer on Si/SiO_2 substrate, then rigid SEBS was applied by stencil printing as the elastiff layer, then soft SEBS was laminated as the stretchable substrate. Subsequently, the dextran sacrificial layer was removed by dissolving in water, then CNT was spray-coated as gate and interconnect electrodes. In this array, the elastiff and substrate layers adhered strongly to each other, because they are both composed of SEBS family but have different butadiene/styrene ratios. As a result, the applied strain was effectively released by the soft substrate that had lower stiffness than the elastiff layer, so $< 10\%$ strain was applied to the device when 100% global strain was applied. In a stretching test at 100% strain, the array's electrical characteristics decreased by $< 5\%$ and maintained carrier mobility after 1000 cycles. This use of an elastiff layer is a promising method to develop high-density stretchable EGOSTs that are highly stable against mechanical deformation. This strategy is expected to realize the practical use of neuromorphic implants.

3.2. Environmental stability

An EGOST for use in interfaces with biological tissues must be environmentally stable *in vivo*. The environmental stability of the implanted EGOST can be mainly assessed in two main aspects: device stability against biofluids, and biocompatibility of component materials. Stability against biofluids is crucial for preventing the body's environment from causing adverse effects on the EGOSTs, which can reduce the device lifetime and thus limit its usability. Biocompatibility assessment is essential because it determines the extent to which an EGOST may cause side effects such as tissue damage. Also, biodegradability, which indicates the biocompatibility of breakdown products of the device after performing its designed functions, is necessary for the development of advanced implants that do not require surgery for removal. Material selection and engineering are needed to simultaneously achieve environmental stability and the required functions of the EGOSTs.

The stability against biofluids requires chemical stability in water, which can degrade the charge-transport properties of organic channels. Additionally, the materials of the device must not be affected by other ambient substances, such as O_2. To maintain mechanical stability while achieving water and ambient stability, the device can be encapsulated in stretchable materials that have mechanical properties that are compatible with biological tissues (Sang et al., 2022). Encapsulation of EGOST devices for stretchable applications has used stretchable polymers such as PDMS (Fig. 4a) (Dai et al., 2022a). The devices composed of a PDMS substrate, stretchable gold electrodes, poly-[3,30-bis(2-(2-(2-methoxyethoxy) ethoxy)ethoxy)2,20-bithiophene] (p(gT2)) channels, and organo-hydrogel, were encapsulated with PDMS. This approach had on-shelf stability >130 d, with the transfer curve remaining almost unchanged. Thus, encapsulation using a stretchable polymer could mitigate the degradation of EGOST in ambient conditions (O_2 and moisture); however, I_{on} still decreased slightly. Though encapsulation using a stretchable polymer can block external moisture and oxygen at a certain degree, the stretchable polymer layer is inherently porous, so it is more permeable to external substances (water permeability $= 10^{-15}$-10^{-18} m^2 s^{-1} Pa^{-1}) than rigid encapsulation materials such as metals, dense plastics, and ceramics (Le Floch et al., 2018; Zheng et al., 2023).

High-density surface fluorination can solve this problem by modifying organic channels to be hydrophobic (Fig. 4b) (Zheng et al., 2023). To modify the surface of the organic channel, polybutadiene azide (BA) molecules were used to form a crosslinked layer of a polymer

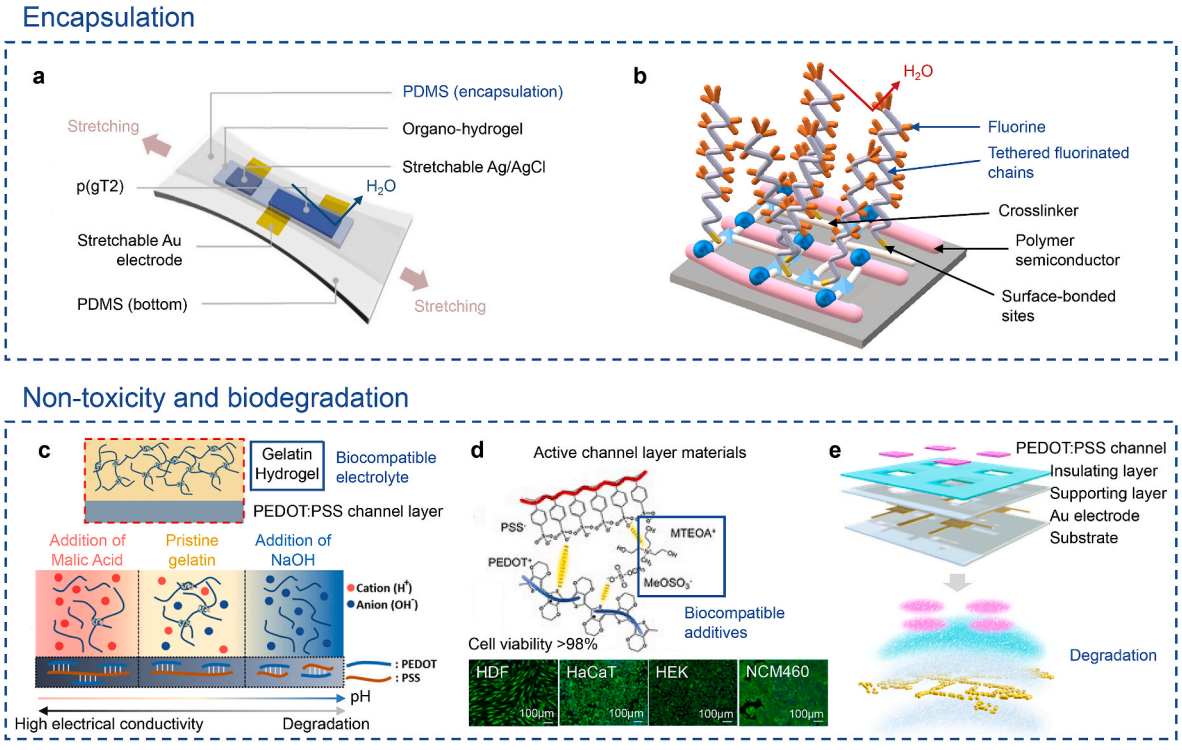

Fig. 4. Methods to increase environmental stability of EGOSTs. **a)** Stretchable polymer encapsulation. Stretchability was maintained while increasing the environmental stability. Reproduced with permission (S. Dai et al., 2022a). Copyright 2022, Elsevier. **b)** Surface modification of polymer semiconductor by tethering fluorinated chains. Molecular hydrophobicity and high fluorination surface density achieved low water permeability of stretchable polymer semiconductor film. Reproduced with permission (Zheng et al., 2023). Copyright 2023, Springer Nature. **c)** The application of gelatin as an electrolyte. The pH of gelatin hydrogel controlled the electrical characteristics of the devices. Reproduced with permission (Jo et al., 2018). Copyright 2018, ACS Publications. **d)** Biocompatible additive, [MTEOA][$MeOSO_3$], to increase electrical conductivity of PEDOT:PSS channel. Human skin cells cultured on PEDOT:PSS/[MTEOA][$MeOSO_3$] films showed high cell viability. Reproduced with permission (Li et al., 2022). Copyright 2022, ACS Publications. **e)** Biodegradable materials that safely break down after use. Devices fabricated from biodegradable materials demonstrated stable operation for a certain period, then degraded autonomously. Reproduced with permission (Wu et al., 2023a). Copyright 2023, Wiley-VCH.

semiconductor, poly-thieno[3,2-*b*]thiophene-diketopyrrolopyrrole (DPPTT), then the surface of the layer was fluorinated by *in situ* tethering of 1H,1H,2H,2H-perfluorodecanethiol (PFDT) molecules. The modified channel remained stretchable, and had water permittivity $<10^{-21}$ m^2 s^{-1} Pa^{-1}, which is lower than that of low-permittivity plastics such as polytetrafluoroethylene (PTFE), polyvinylidene-chloride (PVDC), and parylene (Le Floch et al., 2018; Zheng et al., 2023). A stretchable organic transistor that used the surface-fluorinated organic channel was fabricated using CNT source, drain, and gate electrodes, and SEBS substrate and dielectric layers. This use of PFDT molecules yielded stretchable organic transistors that had high chemical stability when exposed to water and sweat; due to the hydrophobicity of the fluorinated organic channel, the charge-carrier mobility was ~1 cm^2 V^{-1} s^{-1} even when the device was soaked in water and sweat for >30 d. The devices also maintained carrier mobility at both 100% strain and 1000 stretching-releasing cycles at 50% strain, respectively. Therefore, this universal and nanoscale encapsulation method is expected to enable both high environmental and mechanical stability with minimum loss of EGOST function.

Stability of EGOSTs in water and biofluids has been achieved using encapsulation strategies that achieve low water permeability. However, to be useable in implantable devices, EGOST should ensure that it does not induce harmful chemical reactions within the body. Therefore, the use of materials that are biocompatible while maintaining operation and stability is important.

Natural gelatin can be used as a biocompatible electrolyte for electrochemical transistors (Fig. 4c) (Jo et al., 2018). This strategy corresponds to the approach of introducing biomaterials, which has the advantage that it does not require chemical synthesis (Torricelli et al., 2022). Gelatin serves as a semi-solid medium for ion injection, and acids such as malic acid or bases such as NaOH have been added to induce hydrolysis reactions that produce H^+ and OH^-. With gelatin hydrogel that was applied by drop casting, the electrochemical transistor was fabricated by patterning electrodes on a thin polyethylene terephthalate film coated with PEDOT:PSS; the channel was also made of PEDOT:PSS. An electrochemical transistor that used pristine gelatin had a peak g_m ~0.3 mS. The chemical structure and electrical conductivity of the PEDOT:PSS channel vary with the pH of the gelatin hydrogel with additives due to its ion-rich interface. The use of acidic and basic gelatin hydrogels with pH values ranging from 1.13 to 13.43 as electrolytes in electrochemical transistors resulted in an increase and decrease in the electrical conductivity of the PEDOT:PSS channel, attributed to the change in the molecular structure of PEDOT:PSS. For basic gelatin hydrogels with pH above 10, the conductivity of PEDOT:PSS channel decreased due to degradation mechanisms such as ring-opening of polythiophenes and structural change from quinoid to benzoid structure. Therefore, the use of acidic gelatin hydrogels was preferable to the use of basic gelatin hydrogels to ensure both biocompatibility and the electrochemical transistor's functionality. The use of gelatin hydrogel also gave the electrochemical transistor stability against drying, so that it maintained its transfer characteristics for 5 d.

To concurrently increase both the biocompatibility and operation of electrochemical transistors, a strategy of incorporating biocompatible additives into the organic channel has been used (Fig. 4d) (Li et al., 2022). Incorporating the additive tris(2-hydroxyethyl)-methylammonium methylsulfate ([MTEOA][$MeOSO_3$]) into PEDOT:PSS increased its electrical conductivity to > 1000 S cm^{-1}, which was four orders higher than in pristine PEDOT:PSS. This significant improvement was attributed to the enhanced ordering of the PEDOT chains and the formation of nanofibrillar and quinoid structures, which facilitate the creation of conductive paths. In an *in vitro* cytotoxicity test, cell viability on the PEDOT:PSS/[MTEOA][$MeOSO_3$] film toward various human skin cells was over 98% after four days, which indicates that this film is nontoxic to human cells. An electrochemical transistor that used this film was fabricated by patterning gold source and drain electrodes on a parylene substrate, followed by spin-coating with PEDOT:PSS/[MTEOA][$MeOSO_3$] solution. Aqueous NaCl solution was used as the electrolyte, and an Ag/AgCl pellet served as the gate electrode. This electrochemical transistor showed high g_m(NR) = 22.3 (±4.5) mS μm^{-1}, fast response time of about 40.57 μs, and high stability, which maintained over 95% of I_D after 5000 switching cycles. This method is significant in its ability to simultaneously achieve biocompatibility and increase the electrical conductivity of the EGOSTs, although *in vitro* cytotoxicity tests do not necessarily assess biocompatibility *in vivo*,

Another approach is to construct fully-biodegradable devices that perform the intended function stably for a certain period and are then safely absorbed into the body. Such devices eliminate the requirement for surgery to remove the devices; this is a particularly important characteristic for implantable devices that are used for temporary treatment or diagnostic purposes (Li et al., 2020).

A fully-biodegradable electrochemical transistor array that uses PEDOT:PSS was demonstrated by using biodegradable materials (Fig. 4e) (Wu et al., 2023a). It was fabricated using poly(lactic-*co*-glycolic acid) (PLGA) as the biodegradable substrate and insulating layer, and water-soluble polyvinyl alcohol (PVA) as the layer that separated the insulator from the substrate. The device's biodegradability was assessed in a degradation process of electrochemical transistor arrays over time in phosphate-buffered saline (PBS) solution. The array yield was 100% in the first two days, but gradually decreased to 36% by the fourth day. The average g_m was initially 8.9 mS but decreased to 4.0 mS by the sixth day. These results indicate that the electrochemical transistor operated stably for a period of time before degradation, and thus fulfilled the functionality required for a biodegradable device. Subcutaneous implantation of the device into rats for *in vivo* testing achieved a more-precise assessment of its biocompatibility and immune response. The device did not induce visible aggregation of neutrophils, lymphocytes, macrophage cells or granular tissue. This result indicates that surgery for implantation did not stimulate acute inflammation or tissue wounding. This electrochemical transistor has the advantage of being non-toxic and being predominantly composed of biodegradable materials. However, gold was used as the source and drain electrodes, but it has extremely low solubility (0.88–1.74 μg L^{-1}), so additional research should seek alternative materials that can degrade at the desired speed.

3.3. Operational stability

During the operation of EGOST devices, chemical reactions and irreversible microstructural changes caused by swelling can result in the generation of reactive oxygen species that damage biological systems and affect the long-term stability of the device. To ensure the long-term stability and reliability of EGOSTs as implantable devices, these problems must be solved. A great deal of research has introduced molecular design or blending approaches to regulate both desirable and undesirable changes that occur in EGOSTs during their operation, with the goal of controlling the redox process and microstructural evolution (Huang et al., 2023; Szumska et al., 2021; Zhao et al., 2022).

Two reactions determine the operation and stability of EGOSTs: (i) capacitive faradaic reaction and (ii) non-capacitive faradaic reaction. In EGOSTs, capacitive faradaic reactions are doping/de-doping processes of organic channels caused by ions, and are crucial for stable and reversible electrochemical operation. In contrast, non-capacitive faradaic reactions, typically the oxygen reduction reaction (ORR), can produce by-products that can cause degradation of EGOSTs by damaging organic channel materials and harming the biological system (Giovannitti et al., 2020; Xie et al., 2023).

Stabilization of capacitive faradaic reactions in redox-active donor-acceptor polymers while minimizing non-capacitive faradaic reactions can be achieved by designing appropriate molecular structures. This process involves backbone engineering and side-chain engineering to attain an ionization potential (IP) ≥ 4.9 eV; this is the threshold at which the two-electron ORR starts to become endergonic (Fig. 5a) (Giovannitti et al., 2020). Therefore, to investigate the effect of IP, copolymers were

synthesized using glycolated pyridine-flanked diketopyrrolopyrrole (gPyDPP) with bithiophene (p(gPyDPP-T2)), which has IP > 5.3 eV, and with 3,3′-methoxybithiophene (p(gPyDPP-MeOT2)), which has IP = 5.0 eV. Although p(gPyDPP-T2) had IP > 4.9 eV, it had lower electrochemical redox stability than p(gPyDPP-MeOT2); the difference was attributed to the methoxybithiophene (MeOT2) unit providing more localization of the hole polaron than the bithiophene (T2) unit does. These methoxy groups also helped to protect the backbone from side reactions. In the electrochemical transistor fabrication process, chromium/gold bilayer was deposited as the source and drain electrodes, then a parylene C layer and active areas were patterned simultaneously, then coated with polymers. NaCl aqueous solution was used as the electrolyte. The device that used p(gPyDPP-MeOT2) had remarkable stability, with negligible change in I_{on} after 400 cycles at $V_G = -0.5$ V, and only 8% decrease at $V_G = -0.6$ V and 16% decrease at $V_G = -0.7$ V. The electrochemical transistor that used p(gPyDPP-MeOT2) had two orders of magnitude lower I_{off} than electrochemical transistors that used PEDOT:PSS or p(g2T-TT), which are commonly used polymer semiconductors. Also, in conditions of high oxygen concentration, I_{off} of the electrochemical transistor that used p(gPyDPP-MeOT2) changed negligibly, whereas it increased in the devices that used PEDOT:PSS or p(g2T-TT). These results prove that the electrochemical transistor that uses p(gPyDPP-MeOT2) is resilient to ambient conditions. The difference in responses occurs because PEDOT:PSS and p(g2T-TT) facilitate the ORR, which generates H_2O_2. In contrast, p(gPyDPP-MeOT2) does not induce ORR so H_2O_2 does not form. Compared to PEDOT:PSS and p(g2T-TT), which have low IP and are therefore vulnerable to ORR, p(gPyDPP-MeOT2) has a higher IP, and has a significant advantage of stability and safety in aqueous environments. Although the carrier mobility of p(gPyDPP-MeOT2) is only 0.030 (±0.007) $cm^2\ V^{-1}\ s^{-1}$, which is lower than reported in PEDOT:PSS and p(g2T-TT) devices, this strategy of molecular tuning can guide research to inhibit the occurrence of ORR while not degrading the electrochemical doping process of electrochemical transistors.

To simultaneously increase the operational parameters and stability of EGOSTs, high-boiling-point solvents and Lewis acids can be used as semiconductor additives to prevent oxidative degradation due to ORR and to stabilize device operation (Fig. 5b) (Hidalgo Castillo et al., 2022). When tris(pentafluoro phenyl)borane (BCF), a Lewis acid, was added to p(g3T2-T) polymer, which is an all-thiophene polymer with triethylene glycol side chains, the BCF prevents oxidative degradation of the polymer and thereby increase operational stability. To fabricate electrochemical transistors that use p(g3T2-T), chromium/gold bilayer was deposited as the source and drain electrodes, and solutions for the active layer were spin-coated. Aqueous NaCl solution was used as the electrolyte, and an Ag/AgCl pellet was used as the gate electrode. The highest operational stability was observed in the organic channel to which 10 mol% BCF had been added. This result occurred because it can function as a trap site for oxygen molecules, and thereby decrease the ORR. BCF can also relax lamellar structure and generate a flexible network for ion migration. When chlorobenzene (CB), which is a high-boiling-point solvent, was added to the polymer semiconductor, it rearranged the polymer into a hole transport-favorable microstructure and thereby enhanced the transistor parameter. An electrochemical transistor that includes both CB and BCF had $\mu C^* = 556.31$ F $cm^{-1}\ V^{-1}\ s^{-1}$, which is significantly higher than $\mu C^* = 108.31$ F $cm^{-1}\ V^{-1}\ s^{-1}$ in the electrochemical transistor that used pristine film. Additionally, the device with CB and BCF additives had increased stability with a smaller

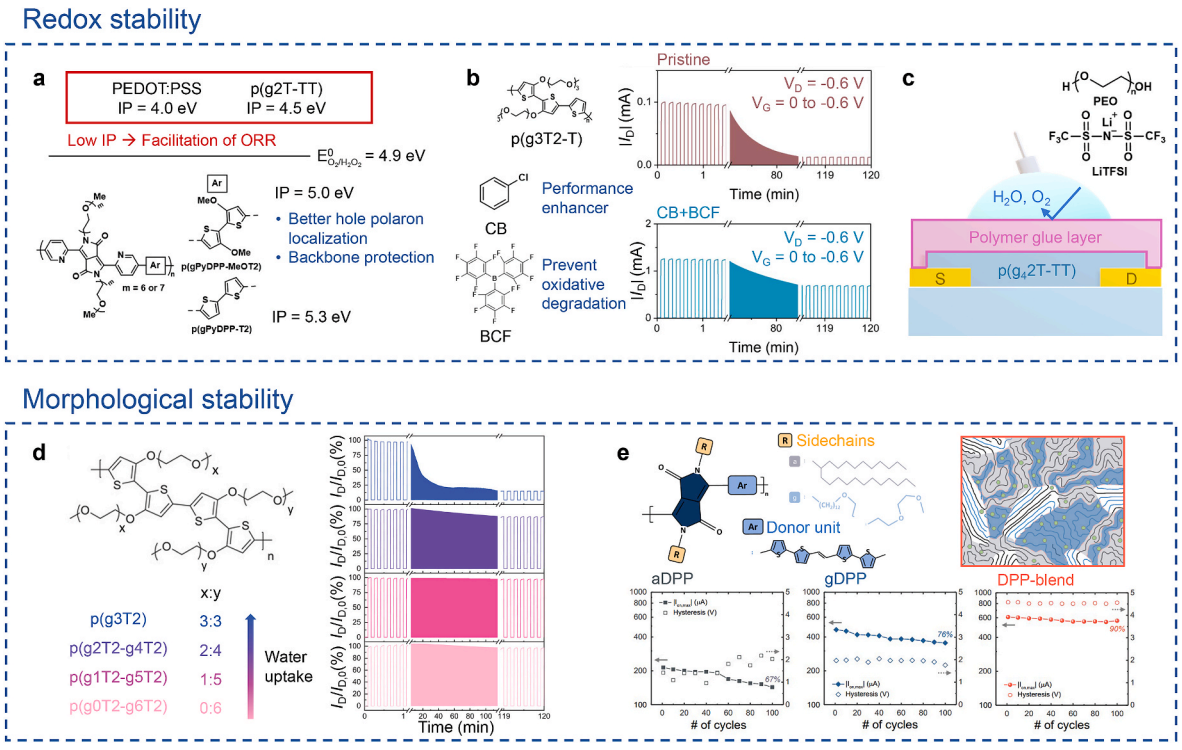

Fig. 5. Methods to increase operational stability of EGOSTs. **a)** Molecular tunning to control IP and increase electrochemical stability. IP > 4.9 eV with hole-polaron localization and backbone protection prevented ORR. Reproduced with permission (Giovannitti et al., 2020). Copyright 2020, Wiley-VCH. **b)** CB and BCF additives to increase operational stability and transistor parameters. BCF prevented oxidative degradation, whereas CB modified crystalline orientation. Reproduced with permission (Hidalgo Castillo et al., 2022). Copyright 2022, ACS Publications. **c)** Polymer glue layer for inhibiting water and oxygen permeation. The polymer glue layer between the organic channel and electrolyte prevented the penetration of water and oxygen and suppressed ORR. Reproduced with permission (Zhang et al., 2023). Copyright 2023, Wiley-VCH. **d)** Redistribution of ethylene glycol side chains to control water uptake. Modifying ethylene glycol side chains to reduce water swelling in polythiophenes increased operational stability. Reproduced with permission (Moser et al., 2020). Copyright 2020, Wiley-VCH. **e)** Blending polymer semiconductors with alkyl and glycol sidechains on the same backbone. Alkyl chains hindered glycol chain expansion, and achieved a robust microstructure, thereby increasing operational stability. Reproduced with permission (Sung et al., 2023). Copyright 2020, Wiley-VCH.

decrease in I_D compared to an electrochemical transistor that only used a CB additive, which degraded completely. Thus, the addition of the additives for polymer rearrangement and suppression of oxidative degradation is a promising strategy to simultaneously increase the stability and transistor parameters of EGOSTs.

Deposition of a polymer glue layer on the semiconductor can significantly increase device stability by effectively preventing the permeation of water and oxygen from the electrolyte layer, which is the cause of the ORR (Fig. 5c) (Zhang et al., 2023). P($g_4$2T-TT), which is a bithiophene-thienothiophene copolymer that has tetraethylene glycol side chains, was used as the channel material of an electrochemical transistor for the application of a polymer glue layer. To fabricate the device, chromium/gold bilayer was deposited as the source and drain electrodes, then polymer film was dissolved in chlorobenzene and applied to the channel by spin-coating. A polymer glue layer, composed of a blend of polyethylene oxide (PEO) and lithium bis(trifluoromethanesulfonyl)imide (LiTFSI), was deposited on the channel. NaCl aqueous solution was used as the electrolyte and Ag/AgCl paste was used as the gate electrode. During stability measurements conducted with gate voltage pulsing between $V_G = 0.15$ V and $V_G = -0.6$ V while maintaining $V_D = -0.6$ V, the I_D in the device without the polymer glue layer fell to <10% of its initial value after 2 h of operation, whereas the device with the polymer glue layer retained 85% of its initial I_D. This result occurred because the polymer glue layer inhibited permeation of water and O_2, and thus suppressed the ORR and consequent formation of OH^-, which contributes significantly to the degradation of the device. Additionally, the use of the polymer glue layer decreased the τ_{ON} from 8 ms to 2 ms; this change was attributed to the increased ionic conductivity that resulted from the dissolution of LiTFSI within the PEO. Interestingly, despite being between the semiconductor and the electrolyte, the glue layer did not affect g_m or I_{on}/I_{off}. Therefore, a polymer glue layer with suitable materials can effectively block water without affecting the doping process.

The use of pendant ethylene glycol (EtG) chains for polymer semiconductors is a promising direction to increase μC^*; this increase is a requirement in EGOSTs with high g_m. Although the above approaches effectively suppress side reactions in these polymer semiconductors, they are susceptible to swelling, which causes irreversible microstructural changes and operational degradation of EGOSTs (Paulsen et al., 2021). To develop neuromorphic implants that operate reliably throughout their lifespan, the effects of swelling must be reduced by suppressing irreversible microstructural changes in polymer films that have EtG side chains. This goal can be achieved by tuning the chemical structure of the polymer semiconductor and optimizing the microstructure of the film.

To overcome the challenge of limited operational stability of polymer semiconductors with EtG side chains, water uptake in the polymer film was optimized using synthesis methods to redistribute EtG side chains. The approach increased both μC^* and the operational stability of the electrochemical transistor (Fig. 5d) (Moser et al., 2020). The effect of EtG side-chain redistribution was investigated by synthesizing four polythiophenes derived from the bithiophene unit with varying lengths of EtG side chains: triethylene glycol (p(g3T2)), alternating diethylene-tetraethylene glycol (p(g2T-g4T)), alternating monoethylene-pentaethylene glycol (p(g1T-g5T)) and alternating methoxy-hexaethylene glycol (p(g0T-g6T)). The hydrophilicity and the ability to stabilize the water molecule in the doped state increased as the EtG chain lengths increased from zero (g0T2) to three (g3T2), but the increase slowed as the number of repeating EtG units exceeded three. Consequently, in the active swelling analysis, the volume of polymer films increased in the following order upon bias application: p(g0T2-g6T2) by 4%, p(g1T2-g5T2) by 10%, p(g2T2-g4T2) by 168%, and p(g3T2) by 249%. To quantify how water swelling correlates with operational stability and steady-state operation, these polythiophenes were deposited on a glass substrate with chromium/gold bilayer as the source and drain electrode, and operated with NaCl aqueous solution as the electrolyte and an Ag/AgCl pellet as the gate electrode. As the polymer's degree of active swelling increased, the operational parameters degraded severely: p(g3T2) retained only 15% of its initial current after more than ~700 cycles (over 2 h) of on-off cycling; the decrease was presumed to be due to the pronounced morphology change. In contrast, p(g0T2-g6T2) and p(g1T2-g5T2) retained 98%, and p(g2T2-g4T2) retained 87%. During steady-state operation p(g1T2-g5T2) had $\mu C^* = 496$ F cm^{-1} V^{-1} s^{-1} and p(g2T2-g4T2) had $\mu C^* = 522$ F cm^{-1} V^{-1} s^{-1}. Therefore, varying the EtG side chain distribution in polythiophenes can overcome the limited operational stability in EGOSTs that use polymer semiconductors with EtG side chains, without compromising μC^*. However, optimization of these side chains necessitates iterative synthesis.

As an alternative, blending polymer semiconductors with alkyl and glycol side chains with the same backbone could also increase operational stability by establishing a robust microstructure (Fig. 5e) (Sung et al., 2023). This possibility was investigated by a comparative study of stability in EGOSTs using three copolymers, each with DPP and thiophene units, but different side chains: alkyl (aDPP), glycol (gDPP), and a blend of these two side chains (DPP-blend). Each polymer was spin-coated on Si/SiO_2 substrate, then gold was deposited by thermal evaporation as the source and drain electrodes, and then PVDF-HFP ion gel was applied as the electrolyte by using a cut-and-paste method. In the DPP-blend, the rigid alkyl side chains of aDPP were adjacent to the flexible EtG side chains of gDPP, where the alkyl chains sterically hindered the expansion of the glycol chains. This relationship preserved the dense π-π backbone stacking crucial for efficient electronic charge transport. After 100 cycles of *I–V* double sweep, the devices that used aDPP or gDPP retained only 67% and 76% of their initial I_{on}, respectively, whereas EGOSTs that used DPP-blend retained 90% of initial I_{on} and showed negligible change in ΔV_{Hys}. Therefore, this well-intermixed DPP-blend film which was obtained by blending polymer semiconductors with alkyl and glycol sidechains on the same backbone, preserved a favorable environment for electronic charge transport and increased operational stability.

4. State-of-the-art neuromorphic implants

EGOSTs may enable the development of neuroprosthetic electronic nerves that emulate the signals and plasticity of biological neurons (Go et al., 2022). This application requires an increase in the stability of functional layer materials to ensure long-term operation without adverse effects on surrounding biological tissues. By implementing the strategies discussed in Section 3 to increase the stability of EGOSTs, practical and long-term useable neuromorphic implants can be fabricated, and may be able to replace biological nerves. This section introduces state-of-the-art neuromorphic implants for the demonstration of neuroprosthetic electronic nerves by adopting strategies for EGOSTs to increase their mechanical and environmental stability.

An artificial perception-actuation loop was demonstrated by using mechanically and environmentally stable EGOST, which had a CONPHINE channel and single-ion conducting polyelectrolyte (Fig. 6a) (Wang et al., 2023b). The EGOST was fabricated using a blend of ionic conducting elastomer (ICE), and photo-patterning polyelectrolyte poly[(1-vinyl-3-propyl-imidazolium) bis(trifluoromethanesulfonyl)imide] (PiTFSI) on a dextran water-soluble sacrificial layer on Si/SiO_2 substrate; then CONPHINE film that used DPP was deposited as the channel, and CNTs were spray-coated as the source and drain electrodes. SEBS/PDMS was applied as a bilayer substrate, then the deposited layers were lifted in water, and CNTs were spray-coated as the gate and interconnect electrodes. The resulting stretchable EGOST maintained a significant ΔV_{Hys} in the transfer curve up to a strain of 50% in both the parallel and perpendicular directions; this result proves its mechanical durability for synaptic behavior. Moreover, the polyelectrolyte could be stably fixed in the elastomer matrix, so fewer ionic species dissolved compared to an electrolyte that used small-molecule ionic liquids

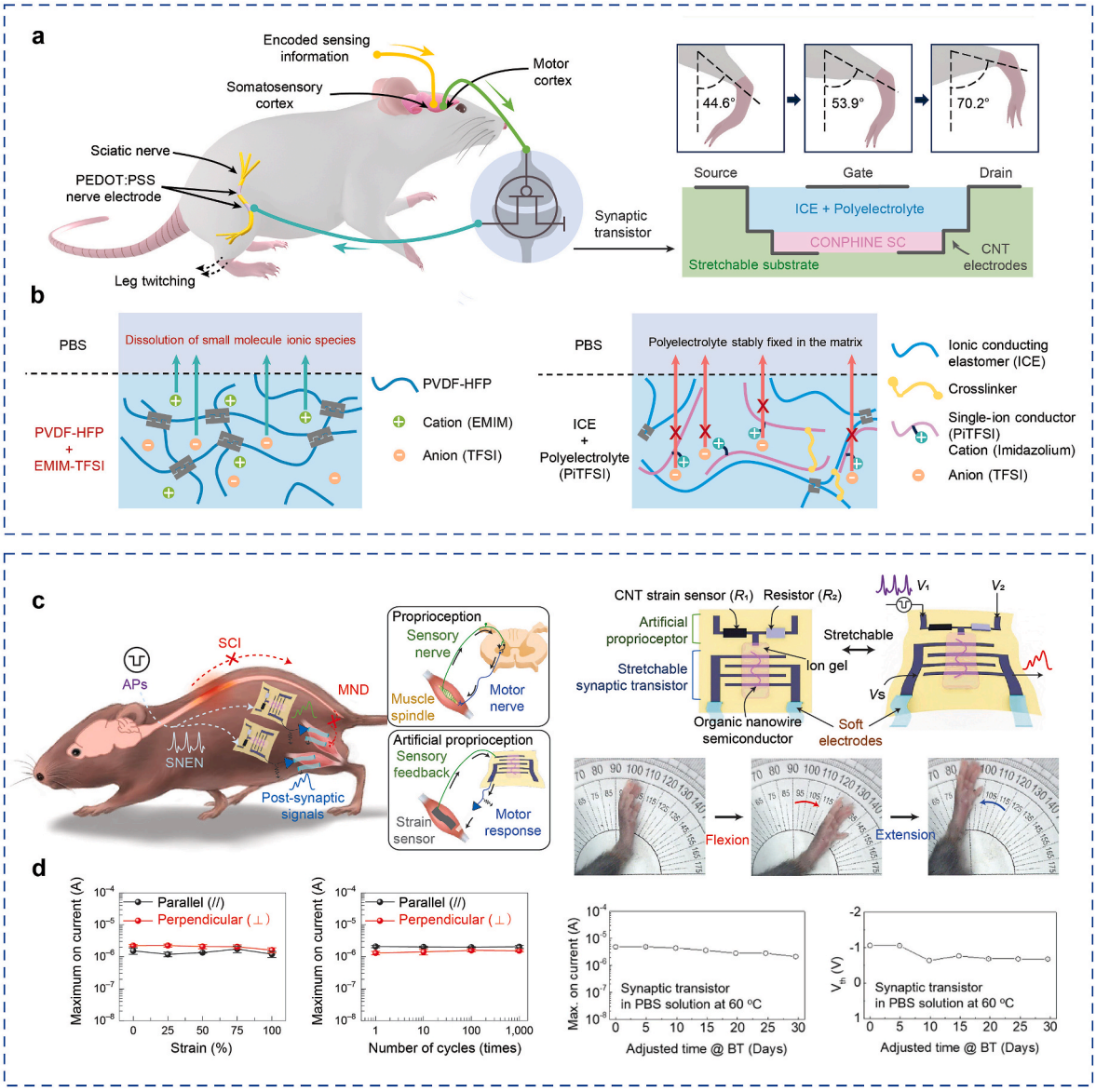

Fig. 6. State-of-the-art neuromorphic implants. **a)** Artificial perception-actuation loop composed of an EGOST that uses a single-ion conducting electrolyte stimulated the sciatic nerve of a live rat to cause leg twitching. **b)** Small-molecule ionic liquids and polyelectrolytes soaked in physiological solution. Reproduced with permission (Wang et al., 2023b). Copyright 2023, AAAS. **c)** Stretchable neuromorphic efferent nerve (SNEN) stimulated the extensor and flexor muscles in the leg of an anaesthetized mouse. **d)** Mechanical and environmental stability of EGOST that uses organic semiconducting nanowires. Reprinted with permission (Lee et al., 2022a). Copyright 2022, Springer Nature.

(Fig. 6b). After being soaked in PBS for 8 h, the EGOST with polyelectrolyte exhibited reduced variation in postsynaptic currents over time, whereas the EGOST that used ionic liquid suffered ~98.2% loss of the initial postsynaptic current. When the EGOST and a stretchable signal conditioning circuit were attached to a live rat, the artificial sensorimotor system converted applied force in a pulse train to stimulate the rat somatosensory cortex, then used the evoked responses from the rat motor cortex as the input of the EGOST. The postsynaptic current of EGOST stimulated the sciatic nerve to cause leg twisting in a live rat, and thereby mimicked a biological sensorimotor loop.

Coordinated leg motion in an anaesthetized mouse could be enabled by a stretchable neuromorphic efferent nerve (SNEN) (Fig. 6c) that used organic semiconducting nanowire-based highly-stretchable EGOST (Lee et al., 2022a). To fabricate a highly-stretchable EGOST, an organic semiconducting nanowire that used a blend of organic semiconductor (FT4-DPP) derived from fused thiophene diketopyrrolopyrrole and SEBS was electro-spun and transferred to a pre-strained SEBS substrate with inter-digitated CNTs as the source and drain electrodes; an ion gel that used poly(styrene-*b*-methyl methacrylate-*b*-styrene) (PS-PMMA-PS) triblock copolymer was drop-cast as the electrolyte. The resulting nanowire-structured organic channel had a serpentine shape that enabled the retention of stable electrical characteristics, so I_{on} was preserved after 1000 cycles of stretching to 100% strain (Fig. 6d).

In the stability test of EGOST in PBS solution, PVDF-HFP ion gel was used instead of PS-PMMA-PS, and the device was encapsulated with PDMS. The resultant device maintained I_{on} and V_{Th} in PBS solution after 6 day at 60 °C; this accelerated aging condition is equivalent to 30 d at body temperature (37 °C). An SNEN was implemented using the EGOST combined with a CNT-based strain sensor to realize artificial proprioception and a soft hydrogel was designed to stimulate the leg muscles of a mouse by using the postsynaptic current of EGOST. The resultant SNEN could stimulate the extensor and flexor muscles in the leg of an anaesthetized mouse, to yield coordinated locomotive motions ('kicking a ball' and 'walking/running'). This result demonstrates the possibility

of using EGOSTs in neuromorphic prosthetic devices.

5. Perspective

Strategies to increase the stability of functional layer materials of EGOSTs could reduce their operational degradation and change in synaptic behavior, which are essential in neuromorphic implants. However, several challenges remain and must be addressed to enable the long-term use of neuromorphic implants in the human body. Therefore, we highlight what state-of-the-art research has achieved and discuss the remaining challenges that must be overcome to achieve this goal (Fig. 7).

Firstly, the development of implantable devices that have long-term stability requires not only tissue-level stretchability (10–70%), but also tissue-level modulus (1–100 kPa) (Li et al., 2021). However, research efforts have been focused on increasing the stretchability, defined as strain-insensitive operation for 1000 cycles of stretching to 100% strain (Lee et al., 2022a). Moreover, stretchable electronic materials and devices still have three to four orders of magnitude higher elastic modulus (above 10 MPa) than most soft biological tissues (below 10 kPa). Therefore, modulus mismatch between the EGOSTs and soft tissues must be reduced by lowering the elastic modulus of EGOSTs to achieve a long-term stable and conformable interface with biological tissues and minimize the effects of mechanical disturbance on device operation (Sunwoo et al., 2021; Li et al., 2023).

Secondly, for practical use, the primary requirement is to evaluate the long-term effects of implantation on the human body, including chronic toxicity and carcinogenicity. For diseases that require long-term implantation, such as spinal cord injury, which requires implantation for up to 10 years (Collinger et al., 2013), long-term *in vivo* evaluation is particularly important. However, reported *in vivo* evaluations of EGOSTs have lasted only a few days (Jo et al., 2020; Wu et al., 2023a). Therefore, to assess the effects of EGOST towards practical use, *in vivo* evaluation must be conducted for several durations: for example, a minimum of 12 months for toxicity testing and 18–24 months for carcinogenicity testing (Combined Chronic Toxicity/Carcinogenicity Studies, 2018), to ensure the medical-grade biocompatibility that is required for clinical translation.

Then, full utilization of EGOST as a temporary medical implant without needing device retrieval surgery will require control of the operational lifetime to be appropriate to the stages of treatment. State-of-the-art biodegradable EGOSTs typically remain intact for only a few days, and extending this lifetime is still an unresearched area. Thus, novel material design concepts must be developed to trigger the degradation mechanism at an on-demand timepoint or to control the degradation kinetics of the biodegradable components (Stephen et al., 2023).

Thirdly, to prevent deterioration in learning accuracy in the long-term, neuromorphic devices must have robust endurance; for instance, towards reliable hardware implementation of artificial neural network (ANN), inference-only accelerators must endure up to 10^6 write events, and training accelerators must endure up to 10^{14} write events (Gumyusenge et al., 2021). The current state-of-the-art EGOST has an endurance of $>2 \times 10^9$ write-read events (equivalent to $> 2 \times 10^7$ full-range cycles) with a 12.8% shift in conductance, which is superior to the endurance of conventional flash memory (10^6 cycles) (Melianas et al., 2020). However, neuromorphic implants do not operate under ideal conditions, so effective strategies to encapsulate EGOSTs must be developed. Additionally, the system-level approach of forgiving (fault tolerant) neural network operations with algorithmic co-development can potentially reduce the fault tolerance requirements to below those of conventional electronics (Gkoupidenis et al., 2023).

Development of long-term stable implantation of EGOSTs must consider these three aspects. For future research, EGOSTs must be integrated with other stretchable circuit components, such as sensors, responding devices, spike processors, and power supplies, in a single unit to enable closed-loop operation for bidirectional signaling with surrounding biological systems (Bruno et al., 2023). The directions of enhancements for EGOSTs that this perspective has presented will allow development of neuromorphic implants that can reliably operate over the demanded duration, and thereby be suitable for practical applications.

6. Conclusion

We have reviewed the structure, working mechanisms, and electrical responses of EGOSTs, and have explored strategies to increase the stability of EGOSTs for neuromorphic implants. Neuromorphic implants comprise a promising method to develop artificial nerves that can be applied for long-term use in a compact system. EGOSTs have been shown to be suitable as components that can emulate synaptic plasticity in a wide range of timescales, so we have discussed their operating mechanisms and classified them according to their dependence on synaptic plasticity. Next, we explained the transistor operational parameters and synaptic behaviors in the spike responses of EGOSTs. The main requirement for practical long-term use of neuromorphic implants is to overcome the instabilities of transistor operation and synaptic behaviors, and the potential adverse effects on the human body. We highlighted methods that can increase the stability of the functional layer material, focusing on electronic and ionic transport, regarding (i) mechanical stability: intrinsic and extrinsic methods, (ii) environmental stability: encapsulation and biocompatibility, and (iii) operational stability: stabilization of redox reaction and morphological change. These methods have demonstrated potential in developing neuromorphic

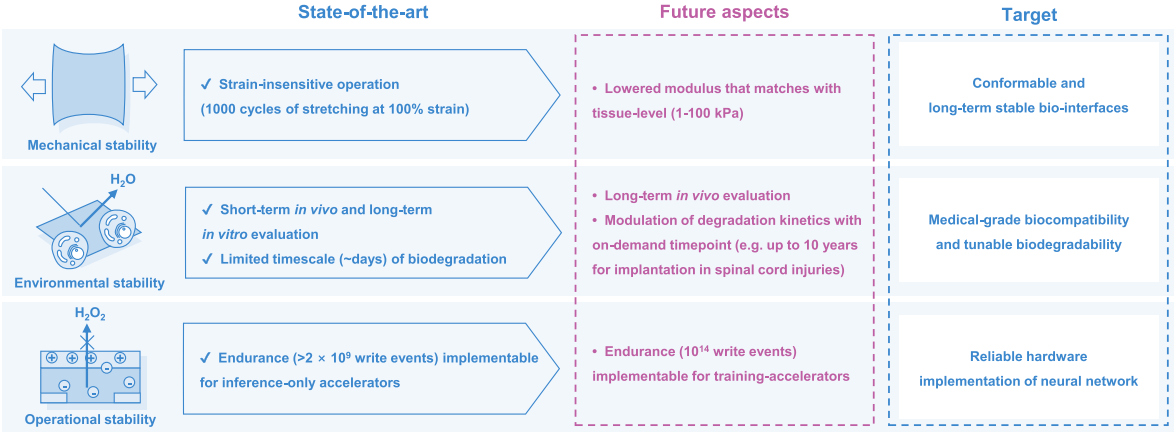

Fig. 7. Perspectives to increase stability in EGOSTs for neuromorphic implants.

implants that can emulate the functionality of the biological nervous system and have the potential to replace damaged nerves. However, research on neuromorphic implants that use EGOST is still in its early stages, so advances beyond the current state-of-the-art are needed. These efforts will help to develop neuromorphic implants that can improve the quality of life for people with medical conditions that require them.

CRediT authorship contribution statement

Seung-Woo Lee: Writing – review & editing, Writing – original draft, Visualization, Project administration, Conceptualization. **Somin Kim:** Writing – review & editing, Writing – original draft, Visualization, Project administration, Conceptualization. **Kwan-Nyeong Kim:** Writing – review & editing, Writing – original draft, Visualization, Project administration, Conceptualization. **Min-Jun Sung:** Writing – review & editing, Writing – original draft, Visualization, Project administration, Conceptualization. **Tae-Woo Lee:** Writing – review & editing, Supervision, Resources, Project administration, Funding acquisition.

Declaration of competing interest

The authors declare the following financial interests/personal relationships which may be considered as potential competing interests: Tae-Woo Lee reports financial support was provided by National Research Foundation of Korea. Seung-Woo Lee reports financial support was provided by National Research Foundation of Korea. Somin Kim reports financial support was provided by National Research Foundation of Korea. Kwan-Nyeong Kim reports financial support was provided by National Research Foundation of Korea. Min-Jun Sung reports financial support was provided by National Research Foundation of Korea. If there are other authors, they declare that they have no known competing financial interests or personal relationships that could have appeared to influence the work reported in this paper.

Data availability

No data was used for the research described in the article.

Acknowledgements

Funding: This work was supported by the National Research Foundation of Korea (NRF) grants funded by Korea government (MSIT) (grant numbers: 2016R1A3B1908431, 2018M3D1A1058536, and 2022M3C1A3081211)

References

Abbott, L.F., Regehr, W.G., 2004. Nature 431, 796–803.
Bazaka, K., Jacob, M.V., 2013. Electronics 2, 1–34.
Bruno, U., Mariano, A., Rana, D., Gemmeke, T., Musall, S., Santoro, F., 2023. Neuromorphic Comput. Eng. 3, 023002.
Chen, J., Huang, W., Zheng, D., Xie, Z., Zhuang, X., Zhao, D., Chen, Y., Su, N., Chen, H., Pankow, R.M., Gao, Z., Yu, J., Guo, X., Cheng, Y., Strzalka, J., Yu, X., Marks, T.J., Facchetti, A., 2022. Nat. Mater. 21, 564–571.
Citri, A., Malenka, R.C., 2008. Neuropsychopharmacology 33, 18–41.
Collinger, J.L., Foldes, S., Bruns, T.M., Wodlinger, B., Gaunt, R., Weber, D.J., 2013. J. Spinal Cord Med 36, 258–272.
Combined Chronic Toxicity/Carcinogenicity Studies (OECD TG 451-3), 2018. In: Revised Guidance Document 150 on Standardised Test Guidelines for Evaluating Chemicals for Endocrine Disruption, OECD Series on Testing and Assessment. OECD, pp. 503–513.
Dai, S., Dai, Y., Zhao, Z., Xia, F., Li, Y., Liu, Y., Cheng, P., Strzalka, J., Li, S., Li, N., Su, Q., Wai, S., Liu, W., Zhang, C., Zhao, R., Yang, J.J., Stevens, R., Xu, J., Huang, J., Wang, S., 2022a. Matter 5, 3375–3390.
Dai, Y., Dai, S., Li, N., Li, Y., Moser, M., Strzalka, J., Prominski, A., Liu, Y., Zhang, Q., Li, S., Hu, H., Liu, W., Chatterji, S., Cheng, P., Tian, B., McCulloch, I., Xu, J., Wang, S., 2022b. Adv. Mater. 34, 2201178.
Giovannitti, A., Rashid, R.B., Thiburce, Q., Paulsen, B.D., Cendra, C., Thorley, K., Moia, D., Mefford, J.T., Hanifi, D., Weiyuan, D., Moser, M., Salleo, A., Nelson, J., McCulloch, I., Rivnay, J., 2020. Adv. Mater. 32, 1908047.
Gkoupidenis, P., Zhang, Y., Kleemann, H., Ling, H., Santoro, F., Fabiano, S., Salleo, A., Van De Burgt, Y., 2023. Nat. Rev. Mater. 9, 134–149.
Go, G.-T., Lee, Y., Seo, D.-G., Pei, M., Lee, W., Yang, H., Lee, T.-W., 2020. Adv. Intell. Syst. 2, 2000012.
Go, G., Lee, Y., Seo, D., Lee, T., 2022. Adv. Mater. 34, 2201864.
Gumyusenge, A., Melianas, A., Keene, S.T., Salleo, A., 2021. Annu. Rev. Mater. Res. 51, 47–71.
Hidalgo Castillo, T.C., Moser, M., Cendra, C., Nayak, P.D., Salleo, A., McCulloch, I., Inal, S., 2022. Chem. Mater. 34, 6723–6733.
Huang, W., Chen, J., Yao, Y., Zheng, D., Ji, X., Feng, L.-W., Moore, D., Glavin, N.R., Xie, M., Chen, Y., Pankow, R.M., Surendran, A., Wang, Z., Xia, Y., Bai, L., Rivnay, J., Ping, J., Guo, X., Cheng, Y., Marks, T.J., Facchetti, A., 2023. Nature 613, 496–502.
Inal, S., Malliaras, G.G., Rivnay, J., 2017. Nat. Commun. 8, 1767.
Ji, X., Paulsen, B.D., Chik, G.K.K., Wu, R., Yin, Y., Chan, P.K.L., Rivnay, J., 2021. Nat. Commun. 12, 2480.
Jo, Y.J., Kwon, K.Y., Khan, Z.U., Crispin, X., Kim, T., 2018. ACS Appl. Mater. Interfaces 10, 39083–39090.
Jo, Y.J., Kim, H., Ok, J., Shin, Y.-J., Shin, J.H., Kim, T.H., Jung, Y., Kim, T., 2020. Adv. Funct. Mater. 30, 1909707.
Kang, J., Mun, J., Zheng, Y., Koizumi, M., Matsuhisa, N., Wu, H.-C., Chen, S., Tok, J.B.-H., Lee, G.H., Jin, L., Bao, Z., 2022. Nat. Nanotechnol. 17, 1265–1271.
Kato, K., Sawada, M., Nishimura, Y., 2019. Nat. Commun. 10, 4699.
Keene, S.T., van der Pol, T.P.A., Zakhidov, D., Weijtens, C.H.L., Janssen, R.A.J., Salleo, A., van de Burgt, Y., 2020. Adv. Mater. 32, 2000270.
Kim, Y., Chortos, A., Xu, W., Liu, Y., Oh, J.Y., Son, D., Kang, J., Foudeh, A.M., Zhu, C., Lee, Y., Niu, S., Liu, J., Pfattner, R., Bao, Z., Lee, T.-W., 2018. Science 360, 998–1003.
Kim, K., Sung, M., Park, H., Lee, T., 2022. Adv. Electron. Mater. 8, 2100935.
Kim, N., Go, G.-T., Park, H.-L., Ahn, Y., Kim, J., Lee, Y., Seo, D.-G., Lee, W., Kim, Y.-H., Yang, H., Lee, T.-W., 2023. Adv. Intell. Syst. 5, 2300016.
Krauhausen, I., Koutsouras, D.A., Melianas, A., Keene, S.T., Lieberth, K., Ledanseur, H., Sheelamanthula, R., Giovannitti, A., Torricelli, F., Mcculloch, I., Blom, P.W.M., Salleo, A., van de Burgt, Y., Gkoupidenis, P., 2021. Sci. Adv. 7, eabl5068.
Le Floch, P., Meixuanzi, S., Tang, J., Liu, J., Suo, Z., 2018. ACS Appl. Mater. Interfaces 10, 27333–27343.
Lee, Y., Lee, T.-W., 2019. Acc. Chem. Res. 52, 964–974.
Lee, Y., Oh, J.Y., Xu, W., Kim, O., Kim, T.R., Kang, J., Kim, Y., Son, D., Tok, J.B.-H., Park, M.J., Bao, Z., Lee, T.-W., 2018. Sci. Adv. 4, eaat7387.
Lee, Y., Park, H.-L., Kim, Y., Lee, T.-W., 2021. Joule 5, 794–810.
Lee, Y., Liu, Y., Seo, D.-G., Oh, J.Y., Kim, Y., Li, J., Kang, J., Kim, J., Mun, J., Foudeh, A. M., Bao, Z., Lee, T.-W., 2022a. Nat. Biomed. Eng. 7, 511–519.
Lee, Y., Oh, J.Y., Lee, T., 2022b. Adv. Mater. Technol. 7, 2200193.
Li, C., Guo, C., Fitzpatrick, V., Ibrahim, A., Zwierstra, M.J., Hanna, P., Lechtig, A., Nazarian, A., Lin, S.J., Kaplan, D.L., 2020. Nat. Rev. Mater. 5, 61–81.
Li, Y., Li, N., De Oliveira, N., Wang, S., 2021. Matter 4, 1125–1141.
Li, T., Cheryl Koh, J.Y., Moudgil, A., Cao, H., Wu, X., Chen, S., Hou, K., Surendran, A., Stephen, M., Tang, C., Wang, C., Wang, Q.J., Tay, C.Y., Leong, W.L., 2022. ACS Nano 16, 12049–12060.
Li, Y., Li, N., Liu, W., Prominski, A., Kang, S., Dai, Y., Liu, Y., Hu, H., Wai, S., Dai, S., Cheng, Z., Su, Q., Cheng, P., Wei, C., Jin, L., Hubbell, J.A., Tian, B., Wang, S., 2023. Nat. Commun. 14, 4488.
Liu, Y.H., Zhu, L.Q., Feng, P., Shi, Y., Wan, Q., 2015. Adv. Mater. 27, 5599–5604.
Liu, G., Guo, Y., Liu, Y., 2024. Matter 7, 430–455.
Lorach, H., Galvez, A., Spagnolo, V., Martel, F., Karakas, S., Intering, N., Vat, M., Faivre, O., Harte, C., Komi, S., Ravier, J., Collin, T., Coquoz, L., Sakr, I., Baaklini, E., Hernandez-Charpak, S.D., Dumont, G., Buschman, R., Buse, N., Denison, T., van Nes, I., Asboth, L., Watrin, A., Struber, L., Sauter-Starace, F., Langar, L., Auboiroux, V., Carda, S., Chabardes, S., Aksenova, T., Demesmaeker, R., Charvet, G., Bloch, J., Courtine, G., 2023. Nature 618, 126–133.
Melianas, A., Quill, T.J., LeCroy, G., Tuchman, Y., Loo, H.V., Keene, S.T., Giovannitti, A., Lee, H.R., Maria, I.P., McCulloch, I., Salleo, A., 2020. Sci. Adv. 6, eabb2958.
Moser, M., Hidalgo, T.C., Surgailis, J., Gladisch, J., Ghosh, S., Sheelamanthula, R., Thiburce, Q., Giovannitti, A., Salleo, A., Gasparini, N., Wadsworth, A., Zozoulenko, I., Berggren, M., Stavrinidou, E., Inal, S., McCulloch, I., 2020. Adv. Mater. 32, 2002748.
Ohayon, D., Druet, V., Inal, S., 2023. Chem. Soc. Rev. 52, 1001–1023.
Park, H.-L., Lee, T.-W., 2021. Org. Electron. 98, 106301.
Park, H., Lee, Y., Kim, N., Seo, D., Go, G., Lee, T., 2020. Adv. Mater. 32, 1903558.
Paulsen, B.D., Fabiano, S., Rivnay, J., 2021. Annu. Rev. Mater. Res. 51, 73–99.
Rivnay, J., Inal, S., Salleo, A., Owens, R.M., Berggren, M., Malliaras, G.G., 2018. Nat. Rev. Mater. 3, 17086.
Sang, M., Kim, K., Shin, J., Yu, K.J., 2022. Adv. Sci. 9, 2202980.
Seo, D.-G., Lee, Y., Go, G.-T., Pei, M., Jung, S., Jeong, Y.H., Lee, W., Park, H.-L., Kim, S.-W., Yang, H., Yang, C., Lee, T.-W., 2019. Nano Energy 65, 104035.
Seo, D.-G., Go, G.-T., Park, H.-L., Lee, T.-W., 2021. MRS Bull. 46, 321–329.
Shim, H., Sim, K., Wang, B., Zhang, Y., Patel, S., Jang, S., Marks, T.J., Facchetti, A., Yu, C., 2023. Nat. Electron. 6, 349–359.
Stephen, M., Nawaz, A., Lee, S.Y., Sonar, P., Leong, W.L., 2023. Adv. Funct. Mater. 33, 2208521.
Sung, M., Seo, D., Kim, J., Baek, H.E., Go, G., Woo, S., Kim, K., Yang, H., Kim, Y., Lee, T., 2023. Adv. Funct. Mater. 2312546.
Sunwoo, S.-H., Ha, K.-H., Lee, S., Lu, N., Kim, D.-H., 2021. Annu. Rev. Chem. Biomol. Eng. 12, 359–391.
Szumska, A.A., Maria, I.P., Flagg, L.Q., Savva, A., Surgailis, J., Paulsen, B.D., Moia, D., Chen, X., Griggs, S., Mefford, J.T., Rashid, R.B., Marks, A., Inal, S., Ginger, D.S., Giovannitti, A., Nelson, J., 2021. J. Am. Chem. Soc. 143, 14795–14805.

Torricelli, F., Alessandri, I., Macchia, E., Vassalini, I., Maddaloni, M., Torsi, L., 2022. Adv. Mater. Technol. 7, 2100445.
Tropp, J., Meli, D., Rivnay, J., 2023. Matter 6, 3132–3164.
van de Burgt, Y., Melianas, A., Keene, S.T., Malliaras, G., Salleo, A., 2018. Nat. Electron. 1, 386–397.
Wang, W., Wang, S., Rastak, R., Ochiai, Y., Niu, S., Jiang, Y., Arunachala, P.K., Zheng, Y., Xu, J., Matsuhisa, N., Yan, X., Kwon, S.-K., Miyakawa, M., Zhang, Z., Ning, R., Foudeh, A.M., Yun, Y., Linder, C., Tok, J.B.-H., Bao, Z., 2021. Nat. Electron. 4, 143–150.
Wang, S., Chen, X., Zhao, C., Kong, Y., Lin, B., Wu, Y., Bi, Z., Xuan, Z., Li, T., Li, Y., Zhang, W., Ma, E., Wang, Z., Ma, W., 2023a. Nat. Electron. 6, 281–291.
Wang, W., Jiang, Y., Zhong, D., Zhang, Z., Choudhury, S., Lai, J.-C., Gong, H., Niu, S., Yan, X., Zheng, Y., Shih, C.-C., Ning, R., Lin, Q., Li, D., Kim, Y.-H., Kim, J., Wang, Y.-X., Zhao, C., Xu, C., Ji, X., Nishio, Y., Lyu, H., Tok, J.B.-H., Bao, Z., 2023b. Science 380, 735–742.
Wang, X., Yang, H., Li, E., Cao, C., Zheng, W., Chen, H., Li, W., 2023c. Small, 2205395.
Wang, Y., Wustoni, S., Surgailis, J., Zhong, Y., Koklu, A., Inal, S., 2024. Nat. Rev. Mater. 1–17.
Wu, M., Yao, K., Huang, N., Li, H., Zhou, J., Shi, R., Li, Jiyu, Huang, X., Li, Jian, Jia, H., Gao, Z., Wong, T.H., Li, D., Hou, S., Liu, Y., Zhang, S., Song, E., Yu, J., Yu, X., 2023a. Adv. Sci. 10, 2300504.
Wu, X., Chen, S., Moser, M., Moudgil, A., Griggs, S., Marks, A., Li, T., McCulloch, I., Leong, W.L., 2023b. Adv. Funct. Mater. 33, 2209354.
Xie, M., Liu, H., Wu, M., Chen, C., Wen, J., Bai, L., Yu, J., Huang, W., 2023. Org. Electron. 117, 106777.
Xu, W., Min, S.-Y., Hwang, H., Lee, T.-W., 2016. Sci. Adv. 2, e1501326.
Xu, J., Wang, S., Wang, G.-J.N., Zhu, C., Luo, S., Jin, L., Gu, X., Chen, S., Feig, V.R., To, J. W.F., Rondeau-Gagné, S., Park, J., Schroeder, B.C., Lu, C., Oh, J.Y., Wang, Y., Kim, Y.-H., Yan, H., Sinclair, R., Zhou, D., Xue, G., Murmann, B., Linder, C., Cai, W., Tok, J.B.-H., Chung, J.W., Bao, Z., 2017. Science 355, 59–64.
Yao, Y., Huang, W., Chen, J., Liu, X., Bai, L., Chen, W., Cheng, Y., Ping, J., Marks, T.J., Facchetti, A., 2023. Adv. Mater. 35, 2209906.
Zhang, S., Ding, P., Ruoko, T.-P., Wu, R., Stoeckel, M.-A., Massetti, M., Liu, T., Vagin, M., Meli, D., Kroon, R., Rivnay, J., Fabiano, S., 2023. Adv. Funct. Mater. 33, 2302249.
Zhao, Y., Su, C., Shen, G., Xie, Z., Xiao, W., Fu, Y., Inal, S., Wang, Q., Wang, Y., Yue, W., McCulloch, I., He, D., 2022. Adv. Funct. Mater. 32, 2205744.
Zheng, Y., Zhang, S., Tok, J.B.-H., Bao, Z., 2022. J. Am. Chem. Soc. 144, 4699–4715.
Zheng, Y., Michalek, L., Liu, Q., Wu, Y., Kim, H., Sayavong, P., Yu, W., Zhong, D., Zhao, C., Yu, Z., Chiong, J.A., Gong, H., Ji, X., Liu, D., Zhang, S., Prine, N., Zhang, Z., Wang, W., Tok, J.B.-H., Gu, X., Cui, Y., Kang, J., Bao, Z., 2023. Nat. Nanotechnol. 18, 1175–1184.
Zucker, R.S., Regehr, W.G., 2002. Annu. Rev. Physiol. 64, 355–405.